

Stein, G. S., Park, W. D., Stein, J. L., & Lieberman, M. W. (1976) *Proc. Natl. Acad. Sci. U.S.A.* 73, 1466-1470.
 Thielmann, H. W. (1976) *Eur. J. Biochem.* 61, 501-513.
 Thielmann, H. W., & Gersbach, H. (1978) *Z. Krebsforsch. Klin. Onkol.* 92, 157-176.

Tlsty, T. D., & Lieberman, M. W. (1978) *Nucleic Acids Res.* 5, 3261-3273.
 Tseng, B. Y., & Goulian, M. (1975) *J. Mol. Biol.* 99, 317-337.
 Yoakum, G. H., & Cole, R. S. (1977) *J. Biol. Chem.* 252, 7023-7030.

Location of the Stilbenedisulfonate Binding Site of the Human Erythrocyte Anion-Exchange System by Resonance Energy Transfer[†]

Anjana Rao,[‡] Paul Martin, Reinhart A. F. Reithmeier,[§] and Lewis C. Cantley*

ABSTRACT: The stilbenedisulfonate inhibitory site of the human erythrocyte anion-exchange system has been characterized by using several fluorescent stilbenedisulfonates. The covalent inhibitor 4-benzamido-4'-isothiocyanostilbene-2,2'-disulfonate (BIDS) reacts specifically with the band 3 protein of the plasma membrane when added to intact erythrocytes, and the reversible inhibitors 4,4'-dibenzamidostilbene-2,2'-disulfonate (DBDS) and 4-benzamido-4'-aminostilbene-2,2'-disulfonate (BADs) show a fluorescence enhancement upon binding to the inhibitory site on erythrocyte ghosts. The fluorescence properties of all three bound probes indicate a rigid, hydrophobic site with nearby tryptophan residues. The Triton X-100 solubilized and purified band 3 protein has similar affinities for DBDS, BADs, and 4,4'-dinitrostilbene-2,2'-disulfonate (DNDS) to those observed on intact erythrocytes and

erythrocyte ghosts, showing that the anion binding site is not perturbed by the solubilization procedure. The distance between the stilbenedisulfonate binding site and a group of cysteine residues on the 40 000-dalton amino-terminal cytoplasmic domain of band 3 was measured by the fluorescence resonance energy transfer technique. Four different fluorescent sulfhydryl reagents were used as either energy transfer donors or energy transfer acceptors in combination with the stilbenedisulfonates (BIDS, DBDS, BADs, and DNDS). Efficiencies of transfer were measured by sensitized emission, donor quenching, and donor lifetime changes. Although these sites are approachable from opposite sides of the membrane by impermeant reagents, they are separated by only 34-42 Å, indicating that the anion binding site is located in a protein cleft which extends some distance into the membrane.

The anion transport system of the human erythrocyte plasma membrane catalyzes bicarbonate for chloride exchange to facilitate CO₂ release in the lungs. A 95 000-dalton polypeptide, labeled band 3 for its relative mobility upon sodium dodecyl sulfate (NaDodSO₄)¹ gel electrophoresis, is responsible for this exchange [for reviews see Cabantchik et al. (1978) and Steck (1978)]. This polypeptide is present in the membrane as a dimer (Steck, 1972; Kiehm & Ji, 1977; Nigg & Cherry, 1979) and makes up approximately 25% of the total membrane protein (Fairbanks et al., 1971). Considerable research on the primary structure has shown that band 3 asymmetrically spans the bilayer with a 40 000-dalton amino-terminal domain in the cytoplasm and a 55 000-dalton carboxy-terminal domain which crosses the bilayer at least once and perhaps several times (Steck et al., 1976; Drickamer, 1976; Rao, 1979).

Although it is clear that this protein catalyzes one for one anion-exchange orders of magnitude faster than unidirectional

transport, the mechanism of this exchange is unknown. Some information about the structure and mechanism of this system has been obtained by using a class of stilbenedisulfonates which are not readily transported but act as high-affinity competitive inhibitors of anion exchange when added to the outside of intact erythrocytes (Maddy, 1964; Cabantchik & Rothstein, 1972, 1974). Two of these compounds, 4,4'-diisothiocyanostilbene-2,2'-disulfonate (DIDS) and 4,4'-diisothiocyanodihydrostilbene-2,2'-disulfonate (H₂-DIDS), react specifically and irreversibly with approximately one site per band 3 monomer to completely inhibit anion exchange in intact erythrocytes (Lepke et al., 1976; Ship et al., 1977; Jennings & Passow, 1979). The reactive site can be approached from the outside of the cell with impermeant reagents (Cabantchik & Rothstein, 1974) and has been located on a 19 000-dalton tryptic fragment near the center of the polypeptide chain (i.e., in the amino-terminal third of the 55 000-dalton carboxy-terminal domain; Grinstein et al., 1978).

In this study we utilize the fluorescent properties of stilbenedisulfonates which interact reversibly [DBDS and BADs; see Table I (a)] or irreversibly (BIDS) with the anion-exchange system to characterize the inhibitory site. The integrity of this site is maintained on red-cell ghosts and on Triton X-100 solubilized and purified band 3. The distance from this site

[†] From the Department of Biochemistry and Molecular Biology, Harvard University, Cambridge, Massachusetts 02138. Received May 11, 1979; revised manuscript received July 11, 1979. This work was supported by Grants GM 26199-01 (L.C.C.) and HL 08893 (Guido Guidotti) from the National Institutes of Health, Grant BMS 73-06752 from the National Science Foundation (Guido Guidotti), and a grant from Research Corporation (L.C.C.).

[‡] Present address: Harvard Medical School, Sidney Farber Cancer Institute, Boston, MA 02115.

[§] Present address: Banting and Best Department of Medical Research, Charles H. Best Institute, University of Toronto.

¹ Abbreviations used: DIDS, 4,4'-diisothiocyanostilbene-2,2'-disulfonate; H₂-DIDS, 4,4'-diisothiocyanodihydrostilbene-2,2'-disulfonate; NaDodSO₄, sodium dodecyl sulfate; all other abbreviations are explained in Table I.

to a group of reactive cysteine residues on the 40 000-dalton cytoplasmic domain (Rao, 1979) is determined by fluorescence resonance energy transfer.

Experimental Section

Materials. 4,4'-Dinitrostilbene-2,2'-disulfonate (DNDS) was purchased from Pfaltz and Bauer. 4,4'-Diaminostilbene-2,2'-disulfonate (DADS) and *N*-[*p*-(2-benzoxazolyl)-phenyl]maleimide were from Eastman. 4,4'-Diisothiocyanostilbene-2,2'-disulfonate (DIDS) and 7-chloro-4-nitrobenz-2-oxa-1,3-diazole (NBD-Cl) were from Pierce Chemical Co. *N*-(3-Pyrene)maleimide was from Regis Chemical Co. Fluorescein-5-maleimide was from Molecular Probes. Triton X-100 was from Rohm and Haas.

Synthesis of Fluorescent Stilbenes. 4,4'-Diaminostilbene-2,2'-disulfonate (14.8 g) was reacted with benzoyl chloride (5.44 g) by the procedure of Kotaki et al. (1971). The product (0.5 g) was applied to a silica gel column (4 × 37 cm) and eluted with a mixture of pyridine-acetic acid-water (10:1:40). Three well-separated peaks absorbing at 340 nm eluted from the column and were analyzed by silica gel thin-layer chromatography (same buffer as the column), UV absorption spectroscopy, and fluorescence spectroscopy. The first peak was identified as unreacted DADS, the second peak was 4-benzamido-4'-aminostilbene-2,2'-disulfonate (BADs), and the third was 4,4'-dibenzamidostilbene-2,2'-disulfonate (DBDS; see Figure 2 for spectral characteristics), in agreement with the results of Kotaki et al. (1971). The DBDS and BADs were recrystallized twice in methanol-water and dried in a desiccator.

4-Benzamido-4'-isothiocyanostilbene-2,2'-disulfonate (BIDS) was synthesized from BADs by using a procedure analogous to that used by Maddy (1964) to synthesize 4-acetamido-4'-isothiocyanostilbene-2,2'-disulfonate (SITS). Briefly, 100 μ L of thiophosgene was added to 50 mg of BADs in 4 mL of 1% NaCl while rapidly vortexing. After a 2-h incubation at 25 °C, the thiophosgene was removed by three 1-mL extractions with diethyl ether. The precipitate was collected, resuspended in 5 mL of 1% NaCl, warmed to dissolve, and crystallized on ice. Crystals were washed with cold water, dried in a desiccator, and kept in the dark. The lysine adduct of BIDS (BIDS-Lys) was formed by reacting 5 mM lysine with 1 mM BIDS at pH 9 for 2 h. The extinction coefficient of this adduct was determined by monitoring the change in the BIDS absorption spectrum as the reaction reached saturation.

Preparation of Red-Cell Ghosts and Fluorescent Labeled Red-Cell Ghosts. Ghosts were prepared from fresh human red cells (from one of the authors) or from newly outdated red cells by standard procedures (Dodge et al., 1973). BIDS-ghosts or DIDS-ghosts were prepared by reacting 200 μ M BIDS or DIDS with 50% intact red cells in pH 8.0 Ringer's solution (145 mM NaCl, 5 mM KCl, 1 mM CaCl₂, 1 mM MgSO₄, and 5 mM sodium phosphate, pH 8.0) at 37 °C for 1 h. Excess reagent was removed by washing 3 times with a fivefold excess of 1% BSA in Ringer's solution. Very little lysis was observed during reaction. Ghosts were then prepared by lysing and washing labeled cells as described above.

NFM-ghosts, NBPM-ghosts, NPM-ghosts, and NFM-BIDS-ghosts were prepared by reacting red-cell ghosts or BIDS-ghosts with 1 mM of the respective maleimide for 1 h at 37 °C in 5 mM sodium phosphate, pH 7.4, with continuous mixing. A low-speed centrifugation (~5 min; 500 rpm) was used to remove any undissolved maleimide. The membranes were then pelleted and washed 3 times with 1%

BSA and 5 mM sodium phosphate, pH 7.4, at 4 °C as described above.

NBD-BIDS-ghosts were prepared by reacting BIDS-ghosts with 1 mM NBD-Cl, using the same procedure as that used for the fluorescent maleimide labeling.

The stoichiometries of the various probes on the red-cell ghosts were determined from a UV-visible absorption scan (Cary 14) of the membranes after dissolving in 1% NaDodSO₄, pH 7.0. The protein concentration was determined by using an absorptivity of 1.09 mL/(mg cm) at 280 nm determined for unmodified ghosts in 1% NaDodSO₄ [this measurement is based on Lowry (1951) protein determination of the same membranes]. The error in protein determination due to probes absorbing at 280 nm is negligible for all probes except NBPM since the other probes have low extinction coefficients at 280 nm. For NBPM-ghosts it was necessary to correct for both the NBPM absorbance at 280 nm ($\epsilon = 1.9 \times 10^4$ M⁻¹ cm⁻¹; Kanaoka et al., 1967) and the protein absorbance at 308 nm [~ 0.04 mL/(mg cm)]. For the other probes, the stoichiometries were determined from the absorbance at the λ_{\max} (after subtracting away protein absorbance) by using the extinction coefficient of the appropriate amino acid adduct (see Table I).

Purification of Band 3 and Fluorescently Labeled Band 3. Red-cell ghosts or labeled red-cell ghosts were depleted of band 6, and a Triton X-100 solubilized extract was applied to a diethylaminoethylcellulose column (0.6 × 5 cm) according to the procedure of Yu & Steck (1975a). [The *p*-(chloromercuri)benzoate treatment was eliminated since this step did not affect the probe specificity of the final protein as judged by NaDodSO₄-polyacrylamide gel electrophoresis.] The column was eluted with 5 mL of 1% Triton X-100 in 44 mM sodium phosphate, pH 8.0, 5 mL of 1% Triton X-100 in 82 mM sodium phosphate, pH 8.0, and 5 mL of 1% Triton X-100 in 170 mM sodium phosphate, pH 8.0, and 0.5-mL fractions were collected. NaDodSO₄-polyacrylamide gel electrophoresis of the fractions revealed that peaks eluting with the 82 and 170 mM buffers were pure in band 3 (see Figure 1). For NFM-band 3, most of the NFM fluorescence and band 3 protein eluted with the 170 mM buffer (probably due to the negatively charged NFM interacting with the column and retarding band 3 elution). The fractions from these columns were collected at 4 °C and were quickly frozen in 100- μ L aliquots with dry ice-acetone and stored at -70 °C to prevent proteolysis.

Since Triton X-100 interferes with protein absorbance at 280 nm and with the Lowry (1951) protein determination, the concentration of purified band 3 protein was determined from 280-nm absorbance scans of 0.5 × 7 cm polyacrylamide gels after electrophoresis in NaDodSO₄. This absorbance was compared with the band 3 absorbance of a series of unstained gels containing various amounts of red-cell ghosts. The total protein concentration in the standards was determined by the Lowry (1951) procedure, and band 3 was assumed to constitute 25% of the total ghost protein (Fairbanks et al., 1971). NaDodSO₄-polyacrylamide gel electrophoresis was done by the procedure of Laemmli (1970).

Inhibition of Phosphate Uptake. [³²P]Phosphate transport into intact red cells was as described by Cantley et al. (1978). Freshly prepared washed red cells were equilibrated with pH 7.4 Ringer's solution at 37 °C. Varying concentrations of DNDS, DBDS, or BADs were added to 50% red cells, followed by a trace of [³²P]phosphoric acid. At 5-min intervals, 1-mL portions of cells were centrifuged for 1 min in a Beckman microfuge. The pellets were washed once with cold Ringer's

solution and then treated with 1 mL of 10% trichloroacetic acid. After again centrifuging, the radioactivity of the supernatant was determined by counting β radiation in Aquasol. Relative transport rates were determined from initial slopes of radioactivity vs. time.

Steady-State Fluorescence. Steady-state fluorescence measurements were performed on either a Foci Mark II spectrofluorometer with corrected excitation or an SLM 4000 polarization spectrofluorometer with a thermostated cell compartment. All measurements were made in 0.3×0.3 cm microcuvettes to minimize inner filter effects and with 1–2.5-nm excitation slits to minimize heating. Shutters were closed between measurements.

In titrations where inner filter effects became significant, a control experiment was performed to determine the inner filter correction. For example, in the case where DNDS quenches NBPM fluorescence by binding to NBPM–band 3, a parallel experiment was performed by using the identical instrument settings and solutions but substituting NBPM–cysteine for NBPM–band 3. At micromolar concentrations, any quenching of NBPM–cysteine fluorescence by DNDS was assumed to be due to inner filter absorption. The fluorescence of NBPM–band 3 at each DNDS concentration was then multiplied by the ratio of NBPM–cysteine fluorescence in the absence of DNDS to that in its presence to give the corrected value. This correction factor was always less than 2 in the concentration range studied.

In titrations where self-quenching of fluorescence was significant, a similar control experiment was performed. For example, to correct for this effect when measuring DBDS fluorescence enhancement upon binding to red-cell ghosts, we performed a parallel experiment using identical solutions and instrument settings but in the absence of ghosts. The fluorescence vs. concentration was linear up to $2\text{--}5 \mu\text{M}$ and then began to curve at higher concentrations due to self-absorbance of exciting or emitting light. A straight line was extrapolated from the linear portion of the data, and the ratio of a point on this straight line to the observed fluorescence at each DBDS concentration was defined as the correction factor. The corresponding data from the ghost titration was multiplied by this factor to obtain the corrected fluorescence. The correction factor was less than two in the concentration range studied. The ΔF in Figures 3–5 is the difference between the corrected fluorescence of probe in the presence of ghosts and that in the absence of ghosts. All titrations were also corrected for dilution effects.

The quantum yield of the various probes bound to ghosts was determined in 5 mM sodium citrate, pH 7.0, at 23°C , by comparison with the quantum yield of quinine sulfate (Parker & Rees, 1966). Equation 1 gives the ratio of quantum

$$Q_1/Q_2 = (F_1/F_2)(A_2/A_1)(1 - r_1/4) \quad (1)$$

yields, Q_i , as a function of the area of the corrected emission spectrum, F_i , and the absorbance at the exciting wavelength, A_i , for two fluorescing compounds where compound 1 is not freely rotating during the excited-state lifetime. The factor $1 - r_1/4$ is a correction for polarized emission (Shinitzky, 1972), and r_1 is the anisotropy of compound 1 (see below). Both A_1 and A_2 were kept below 0.05 absorbance to prevent inner filter effects, and the fluorescence emission was corrected by comparing the spectrum of quinine sulfate on the Foci Mark II to the corrected spectrum (Scott et al., 1970). A quantum yield at 0.70 was used for quinine sulfate in 0.1 N H_2SO_4 at 23°C (Scott et al., 1970).

Fluorescence Anisotropy. Fluorescence anisotropies were measured on an SLM 4000 polarization spectrofluorometer.

This instrument simultaneously measures the ratio of the vertical and horizontal components of emitted light with either the exciting light vertically polarized, $(V/H)_v$, or horizontally polarized, $(V/H)_h$. The anisotropy is defined by eq 2 where

$$r = \frac{(V/H)_v - (V/H)_h}{(V/H)_v + 2(V/H)_h} \quad (2)$$

$(V/H)_h$ corrects for unequal transmission of horizontally and vertically polarized light (Azumi & McGlynn, 1962).

The limiting fluorescence anisotropy (i.e., the anisotropy in the absence of macromolecular rotation), r_{om} , was determined by extrapolating the linear portion of a Perrin plot ($1/r$ vs. T/η) to infinite viscosity as described by Dale & Eisinger (1975). The viscosity was varied by increasing the sucrose concentration at constant temperature (20°C). The fluorescence lifetime was assumed to be independent of sucrose concentration. The dynamic depolarization factor, $(d')_d$, was calculated from the ratio r_{om}/r_f where r_f is the anisotropy in the absence of all rotation (determined by extrapolating the high-viscosity portion of the Perrin plot to infinite viscosity).

Fluorescence Lifetime Measurements. Fluorescence lifetimes were measured on an SLM 4800 lifetime spectrofluorometer with monochromators to select excitation and emission wavelengths. Measurements were made at 23°C in 0.3×0.3 cm microcuvettes. This instrument determines fluorescence lifetimes from phase-shift measurements. For NBPM–band 3, excitation was at 323 nm, emission was at 370 nm, and phase and modulation lifetimes (τ_p and τ_m , respectively) were measured at both 30- and 18-MHz frequencies. For BIDS–band 3, excitation was at 350 nm and emission was monitored with a Kodak W-2C filter. τ_p and τ_m were measured at both 30- and 18-MHz frequencies. For NPM–band 3, excitation was at 344 nm, emission at 381 nm, and 6- and 18-MHz frequencies were used to measure τ_p and τ_m . Light scattering was measured under the same conditions but in the absence of the fluorescent label. (Triton X-100 solutions with minimal fluorescent impurities were used to solubilize band 3). All measurements were made with an excitation polarizer at 55° .

If multiple exponential decays occur in the fluorescent sample, $\tau_p \neq \tau_m$ (Spencer & Weber, 1969). However, for two exponential decays, a unique relation exists between τ_p and τ_m which is dependent on the modulation frequency and the lifetime and amplitudes of the two fluorescent signals. For evaluation of the two exponential decays, a nonlinear least-squares program was written which minimizes the difference between τ_m observed and τ_m theoretical given the observed τ_p at each modulation frequency by varying the two fluorescence decay rates and the ratio of amplitudes. A large number of τ_m and τ_p measurements were made at different frequencies, and the fit was deemed acceptable if the weighted sum of deviations squared (χ^2) was less than the number of data points minus the number of parameters. The program also made corrections for light scattering. A detailed description of this analysis is in preparation.

Fluorescence Resonance Energy Transfer. The efficiency of energy transferred between donor and acceptor molecules was calculated by three procedures. Efficiencies were measured from steady-state fluorescence by donor quenching by using eq 3 where F_{D-A} and F_D are the fluorescence of the

$$E = 1 - F_{D-A}/F_D \quad (3)$$

donor in the presence and absence of the acceptor. Steady-state efficiencies were also measured by sensitized emission of the acceptor by using eq 4.

$$E = \frac{F'_{DA}(\lambda_D, \lambda_A)}{F_{DA}(\lambda_A, \lambda_A)} \frac{A_{DA}(\lambda_A)}{A_{DA}(\lambda_D)} \frac{I(\lambda_A)}{I(\lambda_D)} \quad (4)$$

$F'_{DA}(\lambda_D, \lambda_A)$ is the light emitted by the acceptor on protein containing both donors and acceptors due to energy transfer from the donor and is calculated by eq 5. $F_{DA}(\lambda_A, \lambda_A)$ is the light emitted by the acceptor on protein containing both donor and acceptor upon exciting at the acceptor's maximum absorption wavelength. $A_{DA}(\lambda_A)$ and $A_{DA}(\lambda_D)$ are the absorption of the bound acceptor and bound donor (of the protein containing both species) at their respective maximum absorption wavelengths. $I(\lambda_A)/I(\lambda_D)$ is the ratio of the fluorometer's exciting light intensities at the maximal absorption bands of the acceptor and donor. In order to determine the light emitted at the acceptor wavelength due to energy transfer, it is necessary to subtract away donor emission at the acceptor emission maximum and acceptor excitation at the donor excitation wavelength according to eq 5.

$$F'_{DA}(\lambda_D, \lambda_A) = F_{DA}(\lambda_D, \lambda_A) - F_A(\lambda_D, \lambda_A) - F_D(\lambda_D, \lambda_A) \frac{F_{DA}(\lambda_D, \lambda_D)}{F_D(\lambda_D, \lambda_D)} \quad (5)$$

$F_{DA}(\lambda_D, \lambda_A)$ is the observed fluorescence at the acceptor emission wavelength when exciting a solution of bound donors and acceptors at the donor wavelength. $F_A(\lambda_D, \lambda_A)$ is the same measurement made on an equal concentration of acceptors but in the absence of donors, and $F_D(\lambda_D, \lambda_A)$ is the measurement made in the presence of donors but in the absence of acceptors. $F_{DA}(\lambda_D, \lambda_D)/F_D(\lambda_D, \lambda_D)$ is the ratio of donor intensities of two solutions containing equal bound donor in the presence and absence of acceptor (i.e., the fractional donor quenching due to transfer).

Efficiencies of energy transfer were also calculated from donor fluorescent lifetime measurements in the presence (τ_{DA}) and absence (τ_D) of acceptor by using eq 6.

$$E = 1 - \tau_{DA}/\tau_D \quad (6)$$

The critical transfer distance for a donor-acceptor pair (R_C) was calculated from eq 7.

$$R_C = (9.79 \times 10^3)(J\kappa^2Q_Dn^{-4})^{1/6} \text{ \AA} \quad (7)$$

n is the refractive index of the medium (taken as 1.4 for water), and Q_D is the quantum yield of the donor in the absence of the acceptor. κ^2 is dependent on the orientation of the donor and acceptor transition dipoles and the vector joining them and may vary between 0 and 4. A value of $\kappa^2 = 2/3$ was taken for the calculations in Tables II and IV. The uncertainty in this parameter is discussed below. The overlap integral, J , for the donor emission [$F_D(\lambda)$] and acceptor absorption [$\epsilon_A(\lambda)$] spectra was calculated from eq 8. The summation was carried

$$J = \frac{\sum_{\lambda} F_D(\lambda)\epsilon_A(\lambda)\lambda^4\Delta\lambda}{\sum_{\lambda} F_D(\lambda)\Delta\lambda} \quad (8)$$

out over 10-nm intervals.

Distances between donors and acceptors were calculated from efficiency measurements and critical transfer distances by using the theory of Förster (1959) with the considerations discussed in the Appendix. For reviews of energy transfer in biological systems, see Fairclough & Cantor (1978) and Stryer (1978).

Results

Labeling of Band 3 with BIDS. Intact red cells were reacted

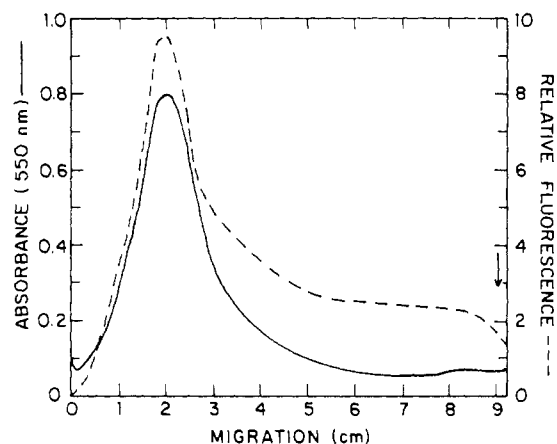


FIGURE 1: The NPM fluorescence intensity (---) and the Coomassie Blue stain intensity (—) of NPM-band 3 after NaDodSO₄-polyacrylamide gel electrophoresis on a 6% gel. Red-cell ghosts were labeled with NPM and band 3 was purified by Triton X-100 extraction as described under Experimental Section. The fluorescence intensity was measured before staining by exciting with 317-nm light and monitoring 90° light intensity of wavelength >380 nm (Kodak W-2C filter) with a fluorescence gel scanner built by Dr. C.-W. Wu.

with BIDS as described under Experimental Section. Ghosts prepared from these cells had 2–2.5 nmol of BIDS incorporated per mg of protein, and 340-nm scans of unstained NaDodSO₄-polyacrylamide gels after electrophoresis revealed that >80% of the BIDS adduct moves at the position of band 3. Band 3 protein was then purified by Triton X-100 extraction of BIDS-labeled ghosts by using the procedure of Yu & Steck (1975a) as outlined under Experimental Section. The 340-nm absorbance of the BIDS adduct copurified with band 3 protein, and the purified protein contained ~10 nmol/mg of BIDS. A NaDodSO₄-polyacrylamide gel electrophoresis pattern of protein purified by this procedure is presented in Figure 1. The absorption maxima of the BIDS moiety of NaDodSO₄-denatured BIDS-ghosts and BIDS-band 3 were at 334 nm, in agreement with that found for the BIDS-Lys adduct (Figure 2A). Before denaturation in NaDodSO₄, the absorption maximum of the BIDS moiety was ~355 nm, and the corrected emission maximum was 435 nm (Figure 2C) for both BIDS-ghosts and BIDS-band 3. These results indicate that, like the analogous reagent DIDS (Lepke et al., 1976), BIDS is highly specific for the band 3 protein when reacting with intact erythrocytes, and the reactive group is probably a lysine residue.

Labeling Cytoplasmic Sulfhydryl Groups of Band 3. In order to determine the distance between the stilbenedisulfonate binding site and a group of reactive cysteine residues on the cytoplasmic surface of band 3 (Rao, 1979), we reacted a number of sulfhydryl reagents with spectral properties appropriate for use as either donors or acceptors of energy transfer with red-cell ghosts or BIDS-ghosts. The three fluorescent maleimides, NFM, NBPM, and NPM, and the reagent NBD-Cl were reacted with ghosts, using conditions (Experimental Section) similar to those used to react *N*-ethylmaleimide with the cytoplasmic SH groups (Rao, 1979). Band 3 was then purified by Triton X-100 extraction as described above, and the stoichiometries of incorporation were determined by absorption scans (Experimental Section). The stoichiometries of incorporation for the various reagents were 10–22 nmol/mg of band 3 protein, and the fluorescent bands on NaDodSO₄-polyacrylamide gels corresponded to the position of band 3 protein (e.g., see Figure 1). The absorption and fluorescence properties of these reagents reacted with sulfhydryl groups are summarized in Table I (b).

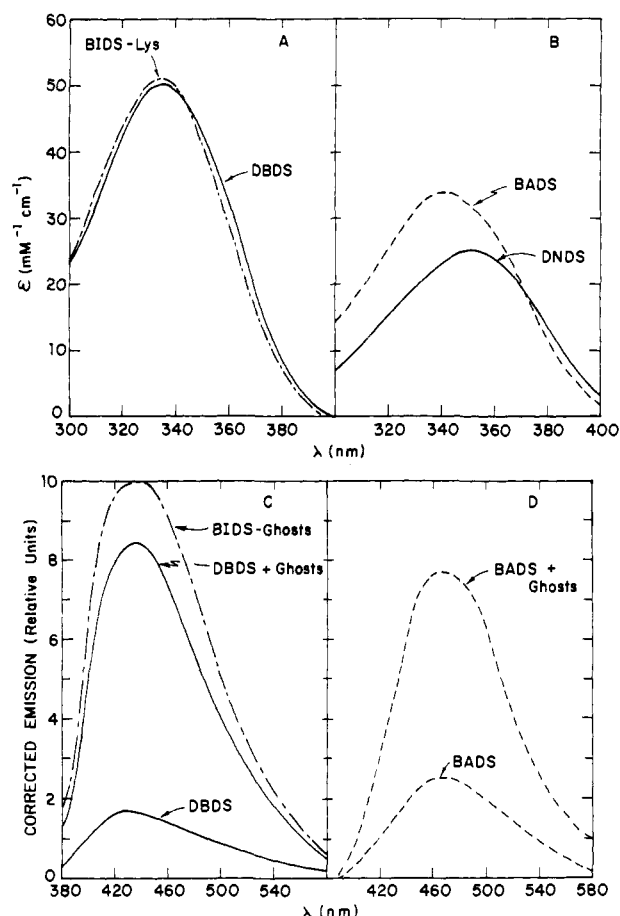


FIGURE 2: (A and B) UV absorption spectra of DBDS, BIDS-Lys, BADS, and DNDS. The compounds were prepared as described under Experimental Section, and all spectra were taken in 5 mM sodium citrate, pH 7.0. (C and D) Fluorescence emission (corrected for the wavelength-dependent photomultiplier response) of BIDS-ghosts, DBDS \pm ghosts, and BADS \pm ghosts. All excitations were at 350 nm, and all measurements were in 0.3 cm by 0.3-cm microcuvettes to minimize inner filter absorption and light scattering. The concentration of DBDS was 1.4 μ M in both cases and BADS was 1.8 μ M in both cases. The red-cell ghost concentration when present was 0.1 mg/mL. The BIDS-ghosts had 2.0 nmol of BIDS per mg of protein. The buffer was 5 mM sodium citrate, pH 7.0, at 23 $^{\circ}$ C. Identical instrument settings were used in the presence and absence of ghosts; however, the relative fluorescence intensities of the different probes may not be compared.

Energy Transfer from BIDS to NFM on Ghosts and Purified Band 3. NFM-BIDS-ghosts were prepared as described above. The fluorescence resonance energy transfer efficiency from BIDS to NFM was found to be 0.47 by sensitized emission as described under Experimental Section. In this procedure one monitors acceptor emission due to donor excitation, and assignment of the fluorescence enhancement to energy transfer is unambiguous. Since the excitation peaks and the emission peaks of this donor-acceptor pair are well separated, there was essentially no background correction and the error in the measurement was less than 10%. The energy transfer efficiency for the same preparation was found to be 0.46 ± 0.05 by measuring donor quenching (see Experimental Section).

The efficiency of energy transferred from BIDS to NFM on band 3 purified from the NFM-BIDS-ghosts was also measured by sensitized emission. In this preparation there was a lower ratio of NFM to BIDS (see Table II), indicating that some of the NFM on ghosts was not bound to band 3; however, the efficiency of transfer was similar to that observed with ghosts ($E = 0.41 \pm 0.04$), suggesting that the NFM groups

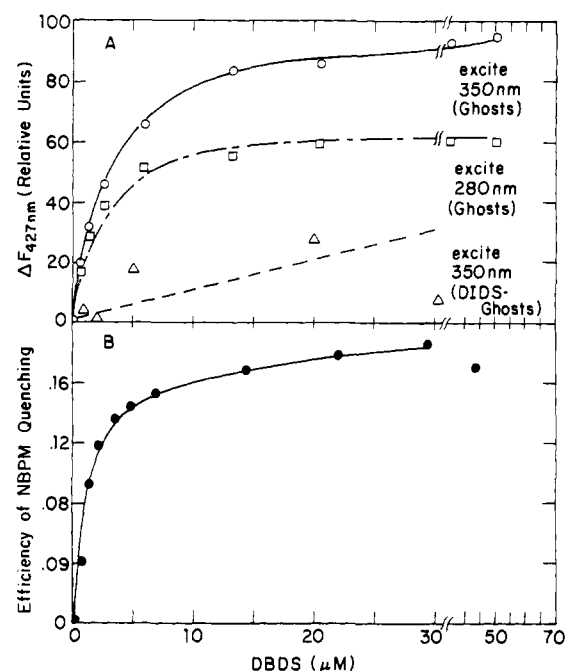


FIGURE 3: (A) Fluorescence enhancement of DBDS upon binding to red-cell ghosts. Excitation was at 350 or 280 nm, and emission was at 427 nm through a Kodac W-2C filter (a Foci Mark II spectrofluorometer with corrected excitation was used). The fluorescence of free DBDS was subtracted away. All three titrations had 0.1 mg/mL ghosts and identical instrument settings. The DIDS-ghosts were prepared by reacting DIDS with intact red cells (Experimental Section). (B) Fractional quenching of NBPM-band 3 fluorescence by DBDS. Excitation was at 310 nm and emission was monitored at 370 nm (no tryptophan or DBDS fluorescence is detectable at these wavelengths). The stoichiometry of NBPM was 14 nmol/mg of protein, and the protein concentration was ~ 0.05 mg/mL in 0.05% Triton X-100 and 5 mM sodium citrate, pH 7.0, at 23 $^{\circ}$ C. All data in (A) and (B) were corrected for inner filter absorption and dilution effects as described under Experimental Section.

acting as acceptors are at a similar distance from the stilbenedisulfonate site in ghosts and purified band 3.

Energy Transfer from BIDS to NBD. NBD-BIDS-band 3 was prepared as described above, and energy transfer efficiencies were measured by donor fluorescence quenching and by donor lifetime changes. These experiments were done by measuring the BIDS fluorescence intensity and lifetime, adding 0.1% 2-mercaptoethanol (which displaces the NBD-S adduct by substitution), and then repeating the measurement. 2-Mercaptoethanol had no effect on BIDS fluorescence in the absence of NBD. The efficiency measured by donor quenching was 0.23 ± 0.05 and that by donor lifetime was 0.14 ± 0.06 . Greater than 99% of the BIDS fluorescence intensity exhibited a single-exponential decay both in the presence and absence of the NBD. These results suggest that all BIDS molecules are similarly quenched by the acceptors (see discussion below).

The stoichiometries of probe incorporation and the energy transfer parameters for BIDS to NFM and BIDS to NBD fluorescence energy transfer are summarized in Table II. The local rotation of probes and donor-acceptor distances are discussed below.

Equilibrium Binding of Fluorescent Stilbenes to Red-Cell Ghosts. In order to determine whether the stilbenedisulfonate site responsible for inhibition of anion exchange is conserved in extensively washed red-cell ghosts, fluorescence experiments were performed by using the noncovalent stilbenedisulfonates DNDS, DBDS, and BADS (Table I). The experiments depicted in parts C and D of Figure 2 show that the weakly fluorescent compounds DBDS and BADS demonstrate con-

Table I

(a) Stilbenedisulfonates						
abbrev	name	R ₁	R ₂	λ _{abs} (nm)	ε _{max} (mM ⁻¹ cm ⁻¹)	λ _{emiss} ^a (nm)
DNDS	4,4'-dinitrostilbene-2,2'-disulfonate	O ₂ N-	-NO ₂	352	25	
DBDS	4,4'-dibenzamidostilbene-2,2'-disulfonate			336	50	435
BADS	4-benzamido-4'-aminostilbene-2,2'-disulfonate		-NH ₂	343	34	465
BIDS	4-benzamido-4'-isothiocyanostilbene-2,2'-disulfonate		-N=C=S	339	62	
BIDS-Lys ^b				334	51	435 ^c
(b) Sulfhydryl Reagents						
abbrev	name	structure	cysteine adduct			
			λ _{abs} (nm)	ε _{max} (mM ⁻¹ cm ⁻¹)	λ _{emiss} (nm)	
NBD-Cl	7-chloro-4-nitrobenz-2-oxa-1,3-diazole		420	13 ^d	540	
fluorescent maleimides						
NBPM	<i>N</i> -[<i>p</i> -(2-benzoxazolyl)phenyl]maleimide		308	32 ^e	370	
NPM	<i>N</i> -pyrenemaleimide		343 325 313	38 ^f	380 400 420	
NFM	<i>N</i> -fluorescein-5-maleimide		488	55 ^g	520	

^a The wavelength of maximum emission (corrected) when bound to band 3. Excitation was at the absorption maximum (λ_{abs}). ^b BIDS reacted with the ε-amino group of *N*-acetyllysine. ^c The maximum emission of BIDS reacted with ghosts. ^d From Birkett et al. (1970). ^e From Kanaoka et al. (1967). ^f ε at 343 nm; from Holowka & Hammes (1977). ^g From the *N*-acetylcysteine adduct of NFM in 5 mM sodium citrate buffer, pH 7.0.

siderable fluorescence enhancement upon addition of red-cell ghosts. A fluorescence titration of ghosts with DBDS (λ_{excit} = 350 nm; λ_{emiss} = 427 nm) is presented in Figure 3A. Double-reciprocal plots of the data are linear, indicating a single class of sites with *K*_d = 2.5 μM. Fluorescence excitation scans (emitting at 427 nm) reveal that, in addition to the 350-nm excitation peak, a 280-nm excitation peak also shows similar enhancement as DBDS binds. Since DBDS does not have an absorption peak at 280 nm and the protein concentration was constant, this peak is apparently due to energy transferred from tryptophan residues to DBDS. The two peaks show parallel saturation, indicating that the DBDS binding site causing fluorescence enhancement is near one or more tryptophan residues.

In order to determine whether the DBDS fluorescence enhancement is due to binding at the site causing transport inhibition, a similar experiment was performed by using ghosts prepared from DIDS-labeled red cells (labeling was done on intact cells, and noncovalent DIDS was removed as described under Experimental Section). An equal concentration of DIDS-labeled ghosts showed only 10–20% as much fluorescence enhancement as unlabeled ghosts (Figure 3A). (Corrections were made for inner filter effects and a weak background fluorescence of DIDS.) Apparently, the fluorescence enhancement results from the externally approachable DIDS binding site responsible for inhibition of anion transport in intact red cells.

A similar fluorescence enhancement titration was performed

Table II: Energy Transfer Parameters with Donor at the Stilbenedisulfonate Site and Acceptor at Cytoplasmic SH Groups^a

Table 10. Energy Transfer Parameters with Donor at the Donor-Sensitizer Site and Acceptor at Cytoplasmic Site Groups																
donor						acceptor				distance						
name	nmol/ mg	Q	τ_0 (ns)	r_{om}	$\langle d' \rangle_d$	name	nmol/ mg	r_{om}	$\langle d' \rangle_d$	R_c (Å)	E	R_1 (Å)	(range)	R_2 (Å)	procedure	
red-cell membranes																
BIDS	2	0.16	0.81	0.345	~1	NFM	8.2	0.22	0.73	34.6	0.47	35	(30–40)	42 ^b	sensitized	
BIDS	2	0.16	0.81	0.345	~1	NFM	8.2	0.22	0.73	34.6	0.46	35	(30–40)	42 ^b	emission donor quenching	
purified band 3																
BIDS	10	0.16	0.81	0.345	~1	NFM	18	0.22	0.73	34.6	0.41	37	(32–42)	40	sensitized	
BIDS	10	0.16	0.81	0.345	~1	NBD	22	<i>c</i>	<i>c</i>	28.5	0.23	35	(29–42) ^d	40	emission donor quenching	
BIDS	10	0.16	0.81	0.345	~1	NBD	22	<i>c</i>	<i>c</i>	28.5	0.14	38	(32–46) ^d	44	lifetime	

^a Symbols used: nmol/mg is the stoichiometry of the probe per protein mass; Q is the quantum yield of bound probe at 23 °C in absence of acceptor; τ_0 is the fluorescence lifetime of bound probe at 23 °C in absence of acceptor; r_{om} is the steady-state anisotropy of bound probe extrapolated to an immobilized macromolecule (see Experimental Section); $\langle d' \rangle_d$ is the average depolarization factor for the bound probe (see Experimental Section); R_c is the critical transfer distance assuming $\kappa^2 = 2/3$; E is the efficiency of energy transfer; R_1 is the donor-acceptor distance, assuming only a single acceptor interacts; (range) represents the most probable limits for R_1 taking into account the uncertainty in κ^2 (see Results); R_2 is the donor-acceptor distance, assuming that all acceptors are equidistant from the donors and that acceptors may occupy up to three sites per band 3 monomer with random occupancy (see Appendix). ^b Assuming all three NFM sites per band 3 monomer are occupied. ^c The NBD-S adduct does not fluoresce sufficiently for accurate polarization measurements. ^d The anisotropy of NBD was assumed to be 0.4, the theoretical maximum.

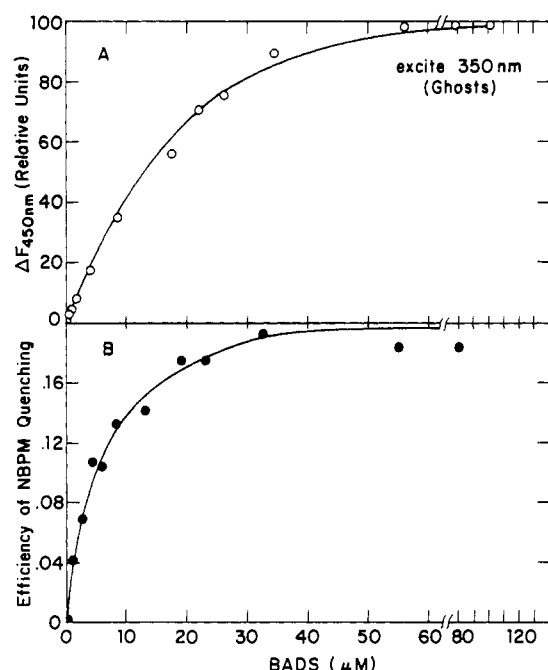


FIGURE 4: (A) Fluorescence enhancement of BADS upon binding to red-cell ghosts. Excitation was at 350 nm and emission was monitored at 450 nm. The ghost concentration was 0.1 mg/mL, and the fluorescence of free BADS was subtracted away. (B) Fractional quenching of NBPM-band 3 fluorescence by BADS. The experimental conditions and data treatment are the same as those described for Figure 3.

by using BADS and red-cell ghosts (Figure 4A). BADS fluorescence also exhibited hyperbolic saturation but revealed a higher dissociation constant than DBDS ($K_d = 13 \mu\text{M}$).

In order to determine whether DBDS, BADS, and the nonfluorescent compound DNDS all compete at the same binding sites on membranes, the enhanced fluorescence of DBDS or BADS on ghosts was monitored while titrating with DNDS (Figure 5A). In both cases, DNDS reduced the enhanced fluorescence by more than 90% with hyperbolic saturation (data were corrected for inner filter absorption by DNDS). This experiment was repeated at a variety of DBDS concentrations, and a plot of $K_{d(\text{app})}$ for DNDS vs. DBDS was linear (data not presented).² From this plot it was determined

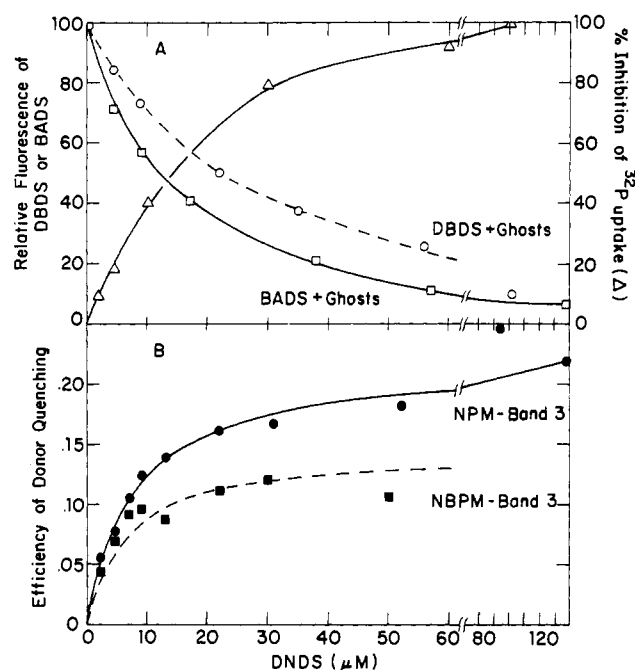


FIGURE 5: (A) Effect of DNDS on membrane-bound DBDS fluorescence (O), membrane-bound BADS fluorescence (□), and [³²P]phosphate uptake by intact red cells (Δ). The DBDS and BADS concentrations were 2.7 and 9.4 μM , respectively, and the red-cell ghost concentration was 0.1 mg/mL (5 mM sodium citrate, pH 7.0, at 23 °C) in both titrations. The DBDS and BADS fluorescence were monitored as described for Figures 3 and 4. Corrections were made for fluorescence of free molecules, inner filter absorption, and dilution effects as described under Experimental Section. Phosphate uptake was measured as described under Experimental Section. (B) Fractional quenching of NBPM-band 3 fluorescence and NPM-band 3 fluorescence by DNDS. The NBPM-band 3 titration was the same as that described in Figure 3B. The NPM-band 3 titration was under identical conditions except that excitation was at 317 nm and emission was monitored at 400 nm.

that the K_d for DNDS is 10 μM and that it competes with a DBDS site of $K_D \sim 2 \mu\text{M}$. The DNDS dissociation constant was also estimated from quenching of intrinsic tryptophan fluorescence (a nearly 50% maximal quenching was apparently

² For competitive binding, $K_{d(\text{app})}(\text{DNDS}) = K_d(\text{DNDS})[1 + (\text{DBDS})/K_d(\text{DBDS})]$.

Table III: Apparent Dissociation Constants for Stilbenedisulfonates

stilbene-disulfonate	$K_{d(\text{app})}$ (μM)	method	source
DBDS	~ 2	inhibition of anion exchange of intact erythrocytes	data not presented ^a
DBDS	2.5	fluorescence enhancement on erythrocyte membranes	Figure 3A
DBDS	2.0	energy transfer from Trp on erythrocyte membranes	Figure 3A
DBDS	1.5	energy transfer from NBPM on purified band 3	Figure 3B
BADS	~ 10	inhibition of anion exchange of intact erythrocytes	data not presented ^a
BADS	13	fluorescence enhancement on erythrocyte membranes	Figure 4A
BADS	5	energy transfer from NBPM on purified band 3	Figure 4B
DNDS	14	inhibition of anion exchange of intact erythrocytes	Figure 5A
DNDS	8	quenching of Trp fluorescence of erythrocyte membranes	data not presented ^b
DNDS	10^c	competition with DBDS on erythrocyte membranes	Figure 5A
DNDS	7^d	competition with BADS on erythrocyte membranes	Figure 5A
DNDS	8	energy transfer from NBPM on purified band 3	Figure 5B
DNDS	6	energy transfer from NPM on purified band 3	Figure 5B

^a Same conditions as DNDS inhibition of [³²P]phosphate uptake presented in Figure 5A. ^b Tryptophan fluorescence was monitored with exciting light at 280 nm and emission at 340 nm. Conditions were the same as those described for Figure 3A. ^c From an extrapolation of $K_{d(\text{app})}$ to (DBDS) = 0. See footnote 2 in the text. ^d From an extrapolation of $K_{d(\text{app})}$ to (BADS) = 0. See footnote 2 in the text.

due to energy transfer as observed with DBDS; data not presented) and from the competition with BADS. The dissociation constants determined are summarized in Table III.

Inhibition of Red-Cell Phosphate Uptake by Stilbenedisulfonates. In order to further demonstrate that the stilbenedisulfonate sites observed in equilibrium experiments are similar to those causing inhibition of anion exchange in red cells, the relative K_1 values for phosphate transport were compared. The percent inhibition of red-cell phosphate uptake vs. extracellular DNDS concentration is plotted in Figure 5A. Inhibition was >99% with hyperbolic saturation and a K_1 of 14 μM . Similar titrations with DBDS and BADS gave K_1 values of 2 and 10 μM , respectively (data not presented). These K_1 values are summarized in Table III along with the equilibrium dissociation constants for red-cell ghosts. Notice that there is excellent agreement between the various constants for a given stilbenedisulfonate and that the order of affinities is DBDS > BADS \approx DNDS.

Equilibrium Binding of Stilbenedisulfonates to Purified Band 3 Measured by Fluorescence Quenching. It was of interest to determine whether band 3 purified by Triton X-100 extraction still maintains its binding site for the stilbenedisulfonate. The Triton X-100 absorbance prevents monitoring binding by tryptophan fluorescence changes, and the fluorescence of impurities in commercial detergent makes DBDS or BADS fluorescence enhancement measurements difficult. However, the sulfhydryl-labeled band 3 preparations (NBPM-band 3 and NPM-band 3; described above) have intense fluorescence properties which may easily be monitored in the presence of Triton X-100. The fluorescence emission of these probes overlaps the absorption of the stilbenedisulfonates (see Table I), allowing energy transfer to occur when the two molecules come within 30–50 Å of each other. The efficiencies of NBPM or NPM fluorescence quenching by DBDS, BADS, and DNDS are plotted as a function of acceptor concentration in Figure 3B, 4B, and 5B, respectively. Notice that the efficiencies of quenching curves saturate hyperbolically and closely parallel the respective fluorescence enhancement curves determined with red-cell ghosts. Apparent dissociation constants were determined from linear double-reciprocal plots of the same data and are summarized in Table III. The close parallel between these dissociation constants and the constants determined for intact red cells and red-cell ghosts shows not only that the stilbenedisulfonate binding sites are still present on solubilized band 3 but also that their dissociation constants and specificities are nearly unchanged

by the solubilization procedure.

Efficiency of Energy Transfer from the Cytoplasmic SH to the Stilbenedisulfonate Site. As explained in the Appendix, considerable information about the arrangement of multiple donors and acceptors may be obtained by reversing the direction of transfer (i.e., placing donors at the SH groups and acceptors at the stilbenedisulfonate site). Thus, the efficiencies measured in Figures 3B–5B, when compared with the data in Table II, provide information about the arrangement of the donor and acceptor sites. In order to verify that the donor fluorescence quenching is due to energy transfer (rather than a conformational change at the donor site) and that the acceptor is at the inhibitory site, we measured energy transfer efficiency from NBPM to DBDS by sensitized emission and from NBPM to BADS (the BADS was covalently attached on intact red cells as described above) by both sensitized emission and donor quenching. Energy transfer from NBPM to DNDS and NPM to DNDS was also measured by donor lifetime changes. NBPM exhibited a single fluorescence lifetime both in the presence (0.70 ns) and in the absence (0.88 ns) of DNDS. NPM fluorescence could be described by two exponential decays with lifetimes of ~ 10 and 83 ns and relative amplitudes of 0.38 and 0.62. In the presence of DNDS, the longer lifetime decreased to 56 ns and the shorter was essentially unchanged. The efficiencies are summarized in Table IV. The good agreement between efficiencies measured by donor quenching and those measured by sensitized emission indicates that most of the quenching observed in Figures 3B–5B is due to energy transfer to the stilbenedisulfonate.

Local Rotational Freedom of Stilbenedisulfonates and Fluorescent Maleimides. In order to determine the distance from the cytoplasmic SH groups to the stilbenedisulfonate site, it is necessary to obtain information about the orientation of the donor and acceptor transition dipoles (i.e., obtain the value for κ^2). The critical transfer distances (R_C) listed in Tables II and IV were calculated by assuming $\kappa^2 = 2/3$ (i.e., the value obtained when donor and acceptor freely rotate during the donor excited-state lifetime). Theoretically, κ^2 may vary from 0 to 4; however, knowledge of the donor and acceptor local rotational freedom (expressed as the dynamic depolarization factor $\langle d' \rangle_d$; see Experimental Section) allows some restriction in the possible values for κ^2 (Dale & Eisinger, 1975). The values of $\langle d' \rangle_d$ are summarized in Tables II and IV. As expected for a high-affinity, specific binding site, the covalently bound BIDS and the noncovalent probes DBDS and BADS showed virtually no detectable local rotation ($\langle d' \rangle_d \approx 1$).

Table IV: Energy Transfer Parameters with Donor on Cytoplasmic SH Groups and Acceptor at the Stilbenedisulfonate Site of Purified Band 3^a

donor						acceptor				distance						procedure
name	nmol/ mg	Q	τ_o (ns)	r_{om}	$\langle d' \rangle_d$	name	nmol/ mg	r_{om}	$\langle d' \rangle_d$	R_C (Å)	E	R_1 (Å)	(range)	R_2 (Å)		
NBPM	15	0.17	0.88	0.238	0.80	BIDS	9.8	0.345	$\sim 1^b$	29.3	0.31	33	(29–38)	37	sensitized emission	
NBPM	15	0.17	0.88	0.238	0.80	BIDS	9.8	0.345	$\sim 1^b$	29.3	0.32	33	(29–38)	37	donor quenching	
NBPM	14	0.17	0.88	0.238	0.80	DBDS	$\sim 10^c$	d	~ 1	29.5	0.38	32	(28–36)	36	sensitized emission	
NBPM	14	0.17	0.88	0.238	0.80	DBDS	~ 10	d	~ 1	29.5	0.19	38	(33–43)	42	donor quenching	
NBPM	14	0.17	0.88	0.238	0.80	BADS	$\sim 10^c$	d	~ 1	29.1	0.20	37	(32–42)	41	donor quenching	
NBPM	14	0.17	0.88	0.238	0.80	DNDS	$\sim 10^c$	d	~ 1	28.7	0.20	36	(31–41)	41	lifetime	
NBPM	14	0.17	0.88	0.238	0.80	DNDS	~ 10	d	~ 1	28.7	0.13	39	(34–44)	44	donor quenching	
NPM	~ 20	0.14	10, 83	0.143	0.70	DNDS	~ 10	d	~ 1	26.5	0.33	30	(26–34)	33	lifetime	
NPM	20	0.14	10, 83	0.143	0.70	DNDS	~ 10	d	~ 1	26.5	0.21	33	(29–37)	37	donor quenching	

^a All symbols are the same as described in Table II except R_2 is calculated, assuming that all donors are interacting equally with two acceptors. Thus, $R_2 = R_1 2^{1/6}$ (see Discussion). ^b No appreciable change in r with viscosity was detected. ^c The noncovalent stilbenedisulfonates are assumed to have the same stoichiometry as BIDS at saturation. ^d Accurate measurements of the viscosity-dependent anisotropy of bound stilbenedisulfonates were complicated by the signal contributed by free molecules [see Cantley & Hammes (1975) for a theoretical treatment]; however, r_{om} was greater than 0.35 for both DBDS and BADS bound to ghosts.

However, the various fluorescent maleimides had dynamic depolarization factors of 0.70–0.80, indicating rotational freedom over the surface of a cone of angle 17° – 21° or over the volume of a cone of angle 23° – 28° (Dale & Eisinger, 1975).

Estimation of the Distance between Cytoplasmic SH Groups and the Stilbenedisulfonate Site. Although the extreme values for κ^2 are not appreciably limited by rotational freedom,³ Hillel & Wu (1976) demonstrate that the probability density function for R/R' (where R' is the donor–acceptor distance calculated by assuming $\kappa^2 = 2/3$, and R is the true distance) is narrowed by the rotational freedom. A similar statistical treatment was used by Haas et al. (1978) to evaluate the most probable range of κ^2 for donors and acceptors of mixed polarization. As pointed out by the authors, this treatment may be extended to probes which show depolarization due to local rotation during the excited-state lifetime or due to a combination of mixed polarization and local rotation. The distances R_1 in Tables II and IV were calculated by assuming $\kappa^2 = 2/3$ and assuming all donors are equally involved in transfer to a single acceptor. The range was determined by dividing R_1 by R'/R at the two half-heights of the probability density function listed in Table III of Haas et al. (1978). The polarizations (p) were calculated from r_{om} for donor and acceptor by using eq 9.

$$p_{om} = 3r_{om}/(2 + r_{om}) \quad (9)$$

If more than one acceptor is close enough to interact with the donor, then the true interaction distance may be longer than R_1 (see the Appendix). The distance R_2 in Table II represents the largest possible distance to the closest SH group and was calculated by using equation A-4 which assumes that up to three equidistant acceptors may interact with the donors.⁴

³ It was possible to further reduce the extreme values for κ^2 by measuring the dynamic transfer depolarization factor $\langle d_T \rangle_d$ for the donor–acceptor pair BIDS–NFM since the sensitized emission was not obscured by background corrections. $\langle d_T \rangle_d$ was estimated to be 0.20 by an extrapolation of the reciprocal anisotropy from the linear portion of a Perrin plot to infinite viscosity. By use of the models described by Dale & Eisinger (1975) with $\theta_{BIDS} = 0^\circ$ and $\theta_{NFM} = 20^\circ$ (surface of cone) or 28° (volume of cone), the extreme values for κ^2 were 0.07 (model 7i) to 3.2 (model 7ii).

⁴ The implied assumption in calculating R_2 in Table II is that energy transfer only occurs between sites on the same monomer. If all six SH groups per dimer are equally involved as acceptors from either donor, then an equation analogous to eq A-4 but with six terms corresponding to the various degrees of saturation is necessary to calculate R . Under conditions of greater than 50% site occupation, it may be approximated that assuming six equidistant acceptors rather than three causes a $2^{1/6}$ increase (or 12%) in the calculated distance.

The number of acceptors (s) was calculated from the stoichiometries by assuming 2.5 nmol of band 3 monomer per mg of ghosts (i.e., 25% of ghost protein is the 95 000 chain) and 10 nmol of band 3 monomer per mg of purified band 3 protein. The distances R_2 in Table IV were calculated by using $R_2 = R_1 2^{1/6}$ which assumes that two equidistant acceptors interact with all the donors (i.e., two BIDS sites per band 3 dimer are equidistant from all the cytoplasmic SH groups).

Notice that R_1 and R_2 were calculated by assuming all donors are similarly quenched by the acceptors. This assumption appears reasonable since a single fluorescence lifetime was observed for the donors BIDS and NBPM in the presence of the acceptors NBD and DNDS⁵ and since efficiencies measured by lifetime changes agreed reasonably with those observed by donor quenching (see Appendix). The average values of R_1 and R_2 in Table II are 36 and 41.6 Å while the average values in Table IV are 34.5 and 38.7 Å. The good agreement among distances calculated by several techniques with several donor–acceptor pairs and by reversing the direction of transfer makes it very unlikely that the true distance between the closest donor–acceptor pair is outside the range of values given.

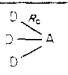
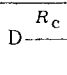
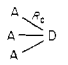
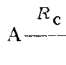
Discussion

The band 3 protein from red-cell membranes has been covalently labeled with the fluorescent stilbenedisulfonate BIDS. The label migrates with band 3 upon NaDodSO₄ gel electrophoresis and copurifies with band 3 protein solubilized in Triton X-100. The stoichiometry of BIDS incorporation is 2–2.5 nmol/mg of ghost protein and 10 nmol/mg of purified band 3, indicating a single site per 95 000-dalton polypeptide chain. The UV absorption of the adduct suggests labeling at a lysine residue, and fluorescence anisotropy measurements indicate a rigid environment for the bound BIDS moiety.

Both red-cell ghosts and purified band 3 protein show reversible specific binding of the noncovalent inhibitors of red-cell anion exchange, DBDS, BADS, and DNDS. All three

⁵ According to eq A-4, at subsaturating values of the acceptor, the donor fluorescence should exhibit multiple fluorescence lifetimes corresponding to zero, one, two, and three acceptors present. However, the BIDS fluorescence in Table II was measured when NBD-Cl had reacted with more than 2/3 of the available sites. It may be calculated by using eq A-4 that 98% of the donors will be in the presence of at least one acceptor and 82% of the donors will be in the presence of either two or three acceptors. The difference between the efficiency of transfer to two or three acceptors is small, making it difficult to resolve the lifetimes. Thus, a single lifetime observed for BIDS in the presence of NBD-Cl does not eliminate energy transfer to multiple acceptor sites.

Table A-I: Energy Transfer Efficiencies Expected from Steady-State and Lifetime Measurements When a Known Stoichiometry of Multiple Donors and Acceptors Interact in Two Extreme Arrangements^a

	all pairs equidistant at $R = R_c$	one pair close at $R = R_c$ and all others distant
donors at multiple sites	 $E_{ss} = 0.5$ $E_{lt} = 0.5$	 $E_{ss} = 0.167$ $E_{lt} = 0^b \text{ and } 0.5$
acceptors at multiple sites	 $E_{ss} = 0.75$ $E_{lt} = 0.75$	 $E_{ss} = 0.5$ $E_{lt} = 0.5$

^a Abbreviations used: R_c is the critical transfer distance; D and A are the donors and acceptors; E_{ss} is the efficiency of energy transfer from steady-state fluorescence measurements (donor quenching or sensitized emission); E_{lt} is the efficiency of energy transfer from excited-state lifetime measurements. ^b Two-thirds of the donors will show no change in their excited-state lifetimes.

compounds appear to compete for the same binding site, and this site may be blocked by reacting intact red cells with the irreversible anion-exchange inhibitor DIDS. This site is characterized by a hydrophobic (i.e., enhanced DBDS and BADS fluorescence; Kotaki et al., 1971) and rigid (high fluorescence anisotropy) environment with nearby tryptophan residues (energy transfer from tryptophan to DBDS). There is a remarkable parallel between the K_i values for anion exchange by intact red cells and the K_d values observed on red-cell ghosts and purified band 3 protein for the three reversible stilbenedisulfonates. Detergent solubilization of band 3 apparently does not affect the integrity of this binding site.

The distance from the stilbenedisulfonate binding site to a group of reactive cysteine residues on the cytoplasmic domain of band 3 (Rao, 1979) was measured by fluorescence resonance energy transfer. The fluorescent maleimides NFM, NBPM, and NPM were in general less reactive than *N*-ethylmaleimide in labeling SH groups on band 3. The stoichiometry of labeling on purified band 3 was 14–20 nmol/mg (1.4–2 mol/mol of polypeptide chain) compared with ~30 nmol/mg (3 mol/mol of polypeptide chain) obtained with *N*-ethylmaleimide under similar conditions (Rao, 1979). These SH groups could also be reacted with the reagent NBD-Cl as judged by appearance of a 420-nm absorbance peak [see Table I (b)]. Distances were estimated by placing a donor at the stilbenedisulfonate site and an acceptor at the cytoplasmic SH groups (Table II) and by placing the donor at the cytoplasmic SH groups with the acceptor at the stilbenedisulfonate site (Table IV). In both cases, the distance between the closest donor-acceptor pair was estimated to be 34–42 Å on purified band 3. The BIDS to NFM distance on red-cell ghosts was similar to that observed on solubilized band 3.

In order to evaluate the significance of the distance calculated, it is useful to consider what is currently known about the tertiary and quaternary structure of band 3. Cross-linking studies indicate that membrane-bound band 3 is a dimer of 95 000 polypeptide chains (Steck, 1972; Kiehm & Ji, 1977; Nigg & Cherry, 1979). The Triton X-100 solubilized band 3 migrates with a protein molecular weight of ~175 000 in sedimentation velocity studies (Clarke, 1975) and may be cross-linked to a dimer with copper phenanthroline (Yu & Steck, 1975b; Reithmeier & Rao, 1979), indicating that the Triton X-100 solubilized protein is also a dimer. Mild digestion of red-cell ghosts with trypsin cleaves band 3 at a site 40 000 daltons from the amino terminus (Steck et al., 1976; Rao & Reithmeier, 1979). This 40 000-dalton domain is water-soluble, is readily separable from the membrane, and is located on the cytoplasmic side of the membrane. The reactive SH groups are in the 40 000-dalton domain (Rao, 1979) while the external DIDS binding site is in the 55 000-dalton domain remaining with the membrane (Grinstein et al., 1978). The lack of knowledge about how far the cytoplasmic SH groups protrude from the membrane makes the exact

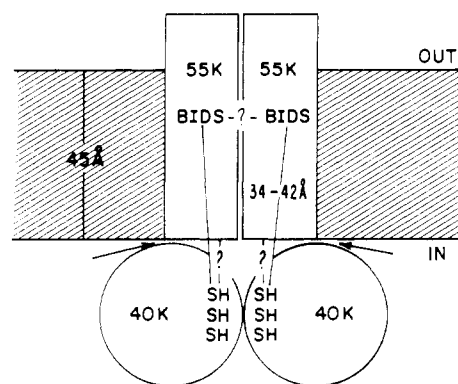


FIGURE 6: Relative location of the stilbenedisulfonate site and cytoplasmic sulfhydryl groups on a band 3 dimer. The 40 000-dalton and 55 000-dalton domains which are separable after a single tryptic cut from the cytoplasmic side of the membrane (arrow) are represented by the circle and rectangle. The dimeric association is assumed to be symmetric. The protein is shown to protrude from both sides of the bilayer as suggested by electron microscopy studies (Weinstein et al., 1978). See the text for an explanation of the distances.

location of the stilbenedisulfonate site uncertain. However, the phosphate head group to head group distance in the red-cell membrane is probably about 45 Å (McCaughan & Krimm, 1979), and a protein sphere of 40 000-dalton mass would have a radius of ~22 Å. Thus, the 34–42-Å distance measured is somewhat shorter than the width of the bilayer, and, depending on the location of the SH group on the 40 000-dalton domain, the externally approachable stilbenedisulfonate site may be near the center of the bilayer or even close to the cytoplasmic side. In any case, the distances measured restrict the location of this site to the inside of the membrane (see Figure 6).

Some discussion of the multiple donor and acceptor arrangements considered in arriving at the distance is warranted. The purified band 3 dimer used for energy transfer experiments had two stilbenedisulfonate sites and ca. three to four labeled cysteine residues. The uncertainty of arrangement complicates a distance measurement. As pointed out in a previous paper (Cantley & Hammes, 1976a) and as discussed in the Appendix, the two extreme values for the closest donor-acceptor distance from a given efficiency measurement are obtained by assuming all interactions occur between a single donor-acceptor pair or assuming all donors and acceptors interact equally (see Table A-I).

Some limitation on the extreme possible arrangements may be made if one exchanges the location of the donor and acceptor and measures energy transfer efficiencies by both steady-state and lifetime techniques. For example, it is unlikely that one of the maleimides is quite close to the stilbenedisulfonate site with the others more distant since this would result in a much shorter distance estimated when BIDS is the donor (Table II) than when NBPM is the donor (Table IV).

Also, a multiple exponential fluorescence decay would be expected for NBPM in the presence of DNDS. Thus, the most likely interpretation of the data is that the difference in distances between the stilbenedisulfonate site and the various SH groups is small compared with the average distance. This interpretation is consistent with the observation that these SH groups may all form interchain disulfide bonds in the presence of copper phenanthroline (Reithmeier & Rao, 1979). In any event, when all donors are equally involved in transfer, then the distance one calculates assuming n equally involved acceptors is $R_1 n^{1/6}$ (i.e., if $n = 3$, then the increase is only 20% greater than the distance calculated by assuming a single acceptor; see eq A-5).

The other major uncertainty in determining a distance is the orientation of the donor and acceptor transition dipoles with respect to the vector joining them. This problem was discussed in some detail under Results. It may be shown from probability density functions (Hillel & Wu, 1976; Haas et al., 1978) that, even though the stilbenedisulfonates are rigidly bound, the local rotation of the maleimides makes it improbable that the distance calculated by assuming $\kappa^2 = 2/3$ is more than 15% in error. In general, it is more likely that the true distance is shorter than the calculated distance than that it is larger. The good agreement between distances measured with four different probes at the SH groups makes it even less likely that the true distance is outside the range estimated.

Finally, the implications of these results for the structure and mechanism of the anion-exchange system should be discussed. Considerable work has been done characterizing the inhibition of red-cell anion exchange by stilbenedisulfonates [for a review see Cabantchik et al. (1978)]. The inhibition is competitive with the anion transported, indicating that these inhibitors bind at the transport site (Shami et al., 1978). However, they do not appear to be transported (Cabantchik & Rothstein, 1974). The equilibrium binding experiments presented here show that not only is the externally approachable transport site conserved in red-cell ghosts but also that it is nearly unchanged in Triton X-100 solubilized and purified band 3. This conclusion is in agreement with circular dichroism studies of Ammonyx LO solubilized band 3 by Yu & Steck (1975a). Thus, structural and mechanistic studies may be more reliably conducted on a well-defined, purified, and solubilized protein.

The fluorescent stilbenes have provided information about the location and environment of the anion recognition site which will be useful in evaluating the mechanism of transport. Quite large molecules (i.e., DBDS) are apparently capable of diffusing some distance into the membrane via a protein cleft to an anion recognition site even though they are not transported. The mechanism by which exchange occurs between this site and the cytoplasm remains obscure.

Added in Proof

A more detailed study of DBDS interaction with red cell membranes shows that binding may be resolved into high and low affinity sites at high ionic strength (J. A. Dix, A. S. Verkman, A. K. Solomon, and L. C. Cantley, unpublished experiments).

Acknowledgments

We thank Guido Guidotti for helpful discussions and part of the financial support for this work. We also thank Alan Kleinfeld for fluorescence lifetime measurements and useful discussions about analysis of multiexponential decays from phase-shift measurements. Cheng-Wen Wu and Zaharia

Hillel are thanked for use of the fluorescence gel scanner.

Appendix

Evaluation of Distances between Multiple Donors and Acceptors. In the case of energy transfer between a single specific site and a group of sites of known stoichiometry, it is possible to estimate the distance from the specific site to the closest site in the group and obtain information about the distribution of distances in the group with appropriate measurements. Table A-I illustrates the two extreme possible arrangements of a group of three sites with respect to a single specific site. In one case the group of sites may lie anywhere on the surface of a sphere of radius R_c with the single specific site at the center of the sphere (energy transfer between donors is assumed not to occur). In the other case one member of the group is close to the specific site and the other members are sufficiently distant so as not to be involved in transfer. It is shown that, although the closest donor-acceptor pair is the same in all arrangements, the observed efficiency of energy transferred is quite sensitive to the arrangement and is dependent on whether the donors or acceptors are at the multiple sites. In one case the apparent efficiencies determined by steady-state (E_{ss}) and lifetime (E_{lt}) measurements differ.

When three donors are equidistant from a single acceptor, all three transfer energy at the same rate (assuming for the purpose of this discussion that donors and acceptors rapidly rotate during the donor excited-state lifetime and that the environments of the donors are similar). Thus, according to Förster (1959)

$$E_{ss} = \frac{\text{energy transferred}}{\text{energy absorbed}} = E_{lt} = 1 - \frac{\tau_{D-A}}{\tau_D} = \frac{(R_c/R)^6}{1 + (R_c/R)^6} \quad (\text{A-1})$$

where τ_{D-A} and τ_D are the donor excited-state lifetimes in the presence and absence of the acceptor. However, if only one of the three donors is involved in transfer, then two-thirds of the donors will have an unperturbed fluorescence and

$$E_{ss} = \frac{\text{energy transferred}}{\text{energy absorbed}} = (1/3) \frac{(R_c/R)^6}{1 + (R_c/R)^6} \quad (\text{A-2})$$

while

$$E_{lt(1)} = 1 - \frac{\tau_{D-A}}{\tau_D} = \frac{(R_c/R)^6}{1 + (R_c/R)^6} \quad (\text{A-3a})$$

$$E_{lt(2)} = 1 - \frac{\tau_D}{\tau_D} = 0 \quad (\text{A-3b})$$

Thus, two lifetimes will be observed, and the efficiency of transfer determined from the shorter lifetime will be 3 times that observed from steady-state measurements.

As shown in the bottom half of Table A-I, additional information is available by exchanging the direction of energy transferred. If acceptors randomly bind to three sites equidistant from a single donor, then it may be shown that [see Cantley & Hammes (1976a) and Matsumoto & Hammes (1975)]

$$E_{ss} = \frac{(R_c/R)^6}{1 + (R_c/R)^6} \frac{s(3-s)^2}{9} + \frac{2(R_c/R)^6}{1 + 2(R_c/R)^6} \frac{s^2(3-s)}{9} + \frac{3(R_c/R)^6}{1 + 3(R_c/R)^6} \frac{s^3}{27} \quad (\text{A-4})$$

where s is the number of acceptor sites occupied. At saturation (i.e., $s = 3$)

$$E_{ss} = E_{lt} = \frac{3(R_c/R)^6}{1 + 3(R_c/R)^6} \quad (\text{A-5})$$

If only one of the three acceptors is involved in transfer, then the efficiency of transfer is proportional to the fractional saturation of sites and at saturation eq A-1 applies. Theoretically, one could distinguish between the two extreme possibilities from a plot of E vs. s ; however, eq A-4 is nearly linear at low values of $(R_c/R)^6$ [see Cantley & Hammes (1976a,b)], making a distinction between the models difficult.

Thus, as illustrated in Table A-I, in either extreme case one always observes a higher efficiency of transfer from steady-state measurements when the donors are at the multiple sites. However, for the single-pair interacting model, placing the acceptors at the multiple sites increases the efficiency of transfer (E_{ss}) by a factor of 3 (note that E_{ss} in eq A-2 is always less than 1/3) while, for the equidistant model, the change in efficiency approaches 0 at high values of $(R_c/R)^6$ and only becomes a factor of 3 when $(R_c/R)^6$ approaches 0. Therefore, from a comparison of the efficiencies measured in the two directions, one may easily determine whether or not one of the donor-acceptor pairs is quite close ($R < R_c$) and, if so, evaluate the distance.

In general, it is difficult to exchange the position of donors and acceptors on a protein since their specific locations are determined by selective binding or selective reaction with functional groups. However, it is often possible to bind a different donor-acceptor pair with a similar R_c which will allow transfer in the opposite direction. In this case it is necessary to compare the values of R obtained using the two extreme models for transfer in each direction. If only one extreme model gives reasonable agreement among distances calculated using both steady-state and lifetime measurements in both directions, then this model can be considered more likely.

References

- Azumi, T., & McGlynn, S. P. (1962) *J. Chem. Phys.* 37, 2413.
- Birkett, D. J., Price, N. C., Radda, G. K., & Salmon, A. G. (1970) *FEBS Lett.* 6, 346.
- Cabantchik, Z. I., & Rothstein, A. (1972) *J. Membr. Biol.* 10, 311.
- Cabantchik, Z. I., & Rothstein, A. (1974) *J. Membr. Biol.* 15, 207.
- Cabantchik, Z. I., Knauf, P. A., & Rothstein, A. (1978) *Biochim. Biophys. Acta* 515, 239.
- Cantley, L. C., & Hammes, G. G. (1975) *Biochemistry* 14, 2968.
- Cantley, L. C., & Hammes, G. G. (1976a) *Biochemistry* 15, 1.
- Cantley, L. C., & Hammes, G. G. (1976b) *Biochemistry* 15, 9.
- Cantley, L. C., Resh, M. D., & Guidotti, G. (1978) *Nature (London)* 272, 552.
- Clarke, S. (1975) *J. Biol. Chem.* 250, 5459.
- Dale, R. E., & Eisinger, J. (1975) in *Biochemical Fluorescence: Concepts* (Chen, R. F., & Edelhoch, H., Eds.) Vol. I, p 115, Marcel Dekker, New York.
- Dodge, J. T., Mitchell, C., & Hanahan, D. T. (1973) *Arch. Biochem. Biophys.* 100, 119.
- Drickamer, L. K. (1976) *J. Biol. Chem.* 251, 5115.
- Fairbanks, G., Steck, T. L., & Wallach, D. F. H. (1971) *Biochemistry* 10, 2606.
- Fairclough, R. H., & Cantor, C. R. (1978) *Methods Enzymol.* 48, 347.
- Förster, T. (1959) *Discuss. Faraday Soc.* 27, 7.
- Grinstein, S., Ship, S., & Rothstein, A. (1978) *Biochim. Biophys. Acta* 507, 294.
- Haas, E., Katzir, E. K., & Steinberg, I. Z. (1978) *Biochemistry* 17, 5065.
- Hillel, Z., and Wu, C.-W. (1976) *Biochemistry* 15, 2105.
- Holowka, D. A., & Hammes, G. G. (1977) *Biochemistry* 16, 5538.
- Jennings, M. L., & Passow, H. (1979) *Biophys. J.* 25, 188a.
- Kanaoka, Y., Machida, M., Ban, Y., & Sekine, T. (1967) *Chem. Pharm. Bull.* 15, 1738.
- Kiehm, D. J., & Ji, T. H. (1977) *J. Biol. Chem.* 252, 8524.
- Kotaki, A., Naoi, M., & Yagi, K. (1971) *Biochim. Biophys. Acta* 299, 547.
- Laemmli, U. K. (1970) *Nature (London)* 227, 680.
- Lepke, S., Fasold, H., Pring, M., & Passow, H. (1976) *J. Membr. Biol.* 29, 147.
- Lowry, O. H., Rosenbrough, N. J., Farr, A. L., & Randall, R. J. (1951) *J. Biol. Chem.* 193, 265.
- Maddy, H. (1964) *Biochim. Biophys. Acta* 88, 390.
- Matsumoto, S., & Hammes, G. G. (1975) *Biochemistry* 14, 214.
- McCaughan, L., & Krimm, S. (1979) *Biophys. J.* 25, 93a.
- Nigg, E., & Cherry, R. J. (1979) *Nature (London)* 277, 493.
- Parker, C. A., & Rees, W. T. (1966) *Analyst (London)* 85, 587.
- Rao, A. (1979) *J. Biol. Chem.* 254, 3053.
- Rao, A., & Reithmeier, R. A. F. (1979) *J. Biol. Chem.* 254, 6144.
- Reithmeier, R. A. F., & Rao, A. (1979) *J. Biol. Chem.* 254, 6151.
- Scott, T. G., Spencer, R. D., Leonard, N. J., & Weber, G. (1970) *J. Am. Chem. Soc.* 92, 687.
- Shami, Y., Rothstein, A., & Knauf, P. A. (1978) *Biochim. Biophys. Acta* 508, 357-363.
- Shinitzky, M. (1972) *J. Chem. Phys.* 56, 5979.
- Ship, S., Shami, Y., Breuer, W., & Rothstein, A. (1977) *J. Membr. Biol.* 33, 311.
- Spencer, R. D., & Weber, G. (1969) *Ann. N.Y. Acad. Sci.* 158, 361.
- Steck, T. L. (1972) *J. Mol. Biol.* 66, 295.
- Steck, T. L. (1978) *J. Supramol. Struct.* 8, 311.
- Steck, T. L., Ramos, B., & Strapazon, E. (1976) *Biochemistry* 15, 1154.
- Stryer, L. (1978) *Annu. Rev. Biochem.* 47, 819.
- Weinstein, R. S., Rhodadad, J. K., & Steck, T. L. (1978) *J. Supramol. Struct.* 8, 325.
- Yu, J., & Steck, T. L. (1975a) *J. Biol. Chem.* 250, 9170.
- Yu, J., & Steck, T. L. (1975b) *J. Biol. Chem.* 250, 9176.